

Two-dimensional Bose plasma in a magnetic field

D. C. Bardos, D. F. Hines, and N. E. Frankel

School of Physics, University of Melbourne, Parkville, Victoria 3052, Australia

(Received 28 October 1992; revised manuscript received 24 June 1993)

We investigate the dielectric response of a planar Bose plasma in the presence of a constant external magnetic field. The conductivity tensor is derived in the self-consistent random-phase approximation. The tensor components are evaluated at zero temperature, leading to explicit dispersion relations for the electrodynamic modes of the plasma. For plasma layers, longitudinal and transverse modes are in general coupled. These coupled modes are investigated in detail.

I. INTRODUCTION

Lower dimensional many-body systems have attracted a great deal of recent interest, particularly in the context of high- T_c superconductivity,¹ which remains one of the major unsolved problems of contemporary physics. The charged Bose gas (CBG) played a central role in the development of a satisfactory theory of conventional superconductivity. In a series of seminal papers, Schafroth² demonstrated the ability of the three-dimensional CBG to display the Meissner effect. This work was later extended to the two-dimensional CBG by May,³ who found that although the two-dimensional CBG did not display a "perfect" Meissner effect, at sufficiently low temperature the system developed an extremely large diamagnetism which amounted to an "imperfect" Meissner effect. May later extended this work to d dimensions.⁴ An excellent historical account of these developments can be found in Blatt.⁵

Current experimental research into high- T_c superconductivity indicates that two-dimensional regions within bulk superconducting structures are responsible for the effect. While the two-dimensional CBG may serve as a model for superconductivity, it also constitutes a fundamental many-body problem and is of major interest in this context.

Research into the dielectric properties of two-dimensional quantum plasmas was initiated in a 1967 paper by Stern⁶ on the dielectric response of the two-dimensional Fermi plasma with zero external magnetic field. Chiu and Quinn⁷ extended this work to include a constant external magnetic field. Fetter considered a hydrodynamic model of the planar electron gas,⁸ which was then generalized to a multiple-layer system, advanced as a model for graphite.⁹ This early work has led to an explosion of interest in lower dimensional many-body systems, which are by now literally a field of their own.^{10,11} The two-dimensional Bose plasma has been studied by Hines and Frankel¹² in the zero-magnetic-field case. Plasmon dispersion, charge screening, and thermodynamic functions near $T=0$ were investigated.

In the present paper, the case of a nonzero external magnetic field is considered. In Sec. II the conductivity tensor is derived in the self-consistent random-phase ap-

proximation (RPA), using techniques introduced by Harris.¹³ In Sec. III the tensor is evaluated for a uniform external magnetic field. At zero temperature, the tensor components can be expressed in terms of Kummer functions. In Sec. IV the results of Sec. III are combined with the dispersion relation for plasma layers, written in terms of the conductivity components,^{7,14} yielding the explicit dispersion relation for the modes of the planar $T=0$ Bose plasma. These modes are then studied in detail analytically and numerically in the high- and low-field limits.

II. CONDUCTIVITY DERIVATION

We now sketch the derivation of the conductivity tensor $\vec{\sigma}$ in the RPA for the two-dimensional boson plasma. The formal development is similar to the approach of Harris.¹³ It is assumed that the response of the system is such that the perturbations to the external fields are small enough to be treated linearly. We write

$$\mathbf{A} = \mathbf{A}_0 + \mathbf{A}_1, \quad \Phi = \Phi_0 + \Phi_1, \quad (1)$$

where \mathbf{A}_0 and Φ_0 are the external potentials, and \mathbf{A}_1 and Φ_1 are small perturbations due to the response of the plasma. The second quantized Hamiltonian for a spin-zero charged Bose field restricted to two dimensions in the presence of an electromagnetic field is written

$$\hat{H} = \int d^2r \hat{\Psi}^\dagger \mathcal{H} \hat{\Psi}, \quad (2)$$

where

$$\mathcal{H} = \frac{1}{2\mu} \left[\mathbf{p} - \frac{e}{c} \mathbf{A} \right]^2 + e\Phi, \quad (3)$$

and μ is the boson mass. The current operator is also required:

$$\mathbf{J}(\mathbf{r}, t) = \frac{e\hbar}{2\mu i} [\hat{\Psi}^\dagger \nabla \hat{\Psi} - (\nabla \hat{\Psi}^\dagger) \hat{\Psi}] - \frac{e^2}{\mu c} \hat{\Psi}^\dagger \hat{\Psi} \mathbf{A}. \quad (4)$$

In the above, $\hat{\Psi}$ is the second quantized Bose field operator:

$$\hat{\Psi} = \sum_{\mathbf{p}} b_{\mathbf{p}}(t) \psi_{\mathbf{p}}(\mathbf{r}), \quad (5)$$

where $b_{\mathbf{p}}(t)$ is the boson annihilation operator for the state \mathbf{p} . The wave functions $\psi_{\mathbf{p}}(\mathbf{r})$ are the boson eigenstates of the unperturbed Hamiltonian $\mathcal{H}_0 = (1/2\mu)[\mathbf{p} - (e/c)\mathbf{A}_0]^2 + e\Phi_0$. An ensemble averaging procedure is employed, similar to that previously used in relativistic conductivity¹⁴ and polarization¹⁵ cal-

culations, leading to an expression for the Fourier transformed current in terms of the electric field \mathbf{E} ,

$$\mathbf{J}(\mathbf{q}, \omega) = \sum_{\mathbf{k}} \vec{\sigma}(\mathbf{q}, \mathbf{k}, \omega) \cdot \mathbf{E}(\mathbf{k}, \omega), \quad (6)$$

from which the conductivity tensor may be obtained:

$$\begin{aligned} \vec{\sigma}(\mathbf{q}, \mathbf{k}, \omega) = & \frac{ie^2}{\mu L^2 \hbar} \sum_{\mathbf{p}, \mathbf{p}'} \frac{F(\mathbf{p}') - F(\mathbf{p})}{\omega - (E_{\mathbf{p}} - E_{\mathbf{p}'})/\hbar + i\eta} \langle \mathbf{p}' | e^{-i\mathbf{q} \cdot \mathbf{r}} \left[\mathbf{p} - \frac{\hbar}{2} \mathbf{q} - \frac{e}{c} \mathbf{A}_0 \right] | \mathbf{p} \rangle \\ & \times \left\{ \langle \mathbf{p} | e^{i\mathbf{k} \cdot \mathbf{r}} | \mathbf{p}' \rangle \frac{\mathbf{k}}{k^2} + \frac{1}{\mu\omega} \langle \mathbf{p} | e^{i\mathbf{k} \cdot \mathbf{r}} \left[\mathbf{p} - \frac{e}{c} \mathbf{A}_0 \right] | \mathbf{p}' \rangle \cdot \left[\vec{\Gamma} - \frac{\mathbf{k}\mathbf{k}}{k^2} \right] \right\} \\ & + \frac{ie^2}{\mu L^2 \omega} \sum_{\mathbf{p}} F(\mathbf{p}) \langle \mathbf{p} | e^{i(\mathbf{k}-\mathbf{q}) \cdot \mathbf{r}} | \mathbf{p} \rangle \left[\vec{\Gamma} - \frac{\mathbf{k}\mathbf{k}}{k^2} \right]. \end{aligned} \quad (7)$$

In the above, $F(\mathbf{p})$ denotes the equilibrium distribution function for the noninteracting Bose gas. The usual two-dimensional matrix elements are employed:

$$\langle \mathbf{p} | \hat{\mathcal{O}} | \mathbf{p}' \rangle e = \int d^2r \psi_{\mathbf{p}}^\dagger \hat{\mathcal{O}} \psi_{\mathbf{p}'}. \quad (8)$$

The tensor (7) is valid for all temperatures and applied electromagnetic fields, the effects of which enter through the distribution functions and matrix elements, respectively. This tensor differs from that of Harris,¹³ where the vector potential term in the current operator (4) was neglected. The conductivity tensor for the three-dimensional plasma can be obtained from the above result, with the substitution of L^3 for L^2 and appropriate interpretation of the matrix elements.

III. TENSOR EVALUATION

We now evaluate the two-dimensional conductivity tensor in the case of a constant external magnetic field perpendicular to the plane. The stationary eigenstates of the Hamiltonian, denoted

$$\psi_{\mathbf{p}}(\mathbf{r}) \equiv \psi_{n, k_x}, \quad \psi_{\mathbf{p}'}(\mathbf{r}) \equiv \psi_{m, k'_x}, \quad (9)$$

are the Landau wave functions

$$\begin{aligned} \psi_{n, k_x} & \equiv N_n \phi_n, \\ \phi_n & = e^{ik_x x - (q_B^2/2)(y+y_0)^2} H_n[q_B(y+y_0)], \\ N_n & = \frac{1}{\sqrt{2^n n! L}} \left[\frac{q_B^2}{\pi} \right]^{1/4}, \end{aligned} \quad (10)$$

where $H_n(x)$ are the Hermite polynomials, and we have used the definitions

$$\begin{aligned} q_B^2 & \equiv \frac{\mu\omega_c}{\hbar}, \\ \omega_c & \equiv \frac{|e|B}{\mu c}, \\ y_0 & \equiv \frac{\hbar c k_x}{eB}. \end{aligned} \quad (11)$$

The corresponding eigenvalues are

$$E_{\mathbf{p}} = E_{n, k_x} = (n + \frac{1}{2}) \hbar \omega_c. \quad (12)$$

To proceed with the evaluation of the conductivity tensor, the following matrix elements are required (see Appendix A for details of derivation):

$$\begin{aligned} \langle \mathbf{p} | e^{i\mathbf{q} \cdot \mathbf{r}} | \mathbf{p}' \rangle & = \delta_{k'_x, k_x - q_x} e^{-(\hbar/\mu\omega_c)\{(1/4)(q_x'^2 + q_y'^2) + i \operatorname{sgn}(e)[q_y' k_x - (1/2)q_x' q_y']\}} F_m(q'), \\ \langle \mathbf{p}' | e^{-i\mathbf{q} \cdot \mathbf{r}} \left[\mathbf{p} - \frac{\hbar}{2} \mathbf{q} - \frac{e}{c} \mathbf{A} \right] | \mathbf{p} \rangle & = \delta_{k'_x, k_x - q_x} e^{-(\hbar/\mu\omega_c)\{(1/4)(q_x^2 + q_y^2) - i \operatorname{sgn}(e)[q_y k_x - (1/2)q_x q_y]\}} \mathbf{M}_1(q), \\ \langle \mathbf{p} | e^{i\mathbf{q} \cdot \mathbf{r}} | \mathbf{p}' \rangle \frac{\mathbf{q}'}{q'^2} + \frac{1}{\mu\omega} \langle \mathbf{p} | e^{i\mathbf{q} \cdot \mathbf{r}} \left[\mathbf{p} - \frac{e}{c} \mathbf{A} \right] | \mathbf{p}' \rangle \cdot \left[\vec{\Gamma} - \frac{\mathbf{q}'\mathbf{q}'}{q'^2} \right] & \\ & = \delta_{k'_x, k_x - q_x} e^{-(\hbar/\mu\omega_e)\{(1/4)(q_x'^2 + q_y'^2) + i \operatorname{sgn}(e)[q_y' k_x - (1/2)q_x' q_y']\}} \mathbf{M}_2(q'), \end{aligned} \quad (13)$$

where $\operatorname{sgn}(e) = \pm 1$ is the sign of the charge, and

$$\mathbf{M}_1(q) = \begin{Bmatrix} \text{sgn}(e)\sqrt{\frac{1}{2}\hbar\mu\omega_c}[\sqrt{n}{}^{n-1}F_m^*(q) + \sqrt{n+1}{}^{n+1}F_m^*(q)] - \frac{1}{2}\hbar q_x {}^nF_m^*(q) \\ i\sqrt{\frac{1}{2}\hbar\mu\omega_c}[\sqrt{n+1}{}^{n+1}F_m^*(q) - \sqrt{n}{}^{n-1}F_m^*(q)] - \frac{1}{2}\hbar q_y {}^nF_m^*(q) \end{Bmatrix}, \tag{14}$$

$$\mathbf{M}_2(q') = {}^nF_m(q') \frac{q'}{q'^2} + \frac{1}{\mu\omega} \begin{Bmatrix} \left[1 - \frac{q_x'^2}{q'^2}\right] \text{sgn}(e)\sqrt{\frac{1}{2}\hbar\mu\omega_c}[\sqrt{m}{}^mF_{m-1}(q') + \sqrt{m+1}{}^mF_{m+1}(q')] \\ - \frac{q'_x q'_y}{q'^2} i\sqrt{\frac{1}{2}\hbar\mu\omega_c}[\sqrt{m+1}{}^mF_{m+1}(q') - \sqrt{m}{}^mF_{m-1}(q')] \\ \left[1 - \frac{q_y'^2}{q'^2}\right] i\sqrt{\frac{1}{2}\hbar\mu\omega_c}[\sqrt{m+1}{}^mF_{m+1}(q') - \sqrt{m}{}^mF_{m-1}(q')] \\ - \frac{q'_x q'_y}{q'^2} \text{sgn}(e)\sqrt{\frac{1}{2}\hbar\mu\omega_c}[\sqrt{m}{}^mF_{m-1}(q') + \sqrt{m+1}{}^mF_{m+1}(q')] \end{Bmatrix},$$

where we have used the definition

$${}^nF_m(q) = \begin{cases} \left[\frac{2^m m!}{2^n n!}\right]^{1/2} \left[\frac{\hbar}{\mu\omega_c}\right]^{(n-m)/2} [q_x \text{sgn}(e) + iq_y]^{n-m} L_m^{n-m} \left[\frac{\hbar}{2\mu\omega_c}(q_x^2 + q_y^2)\right], & m \leq n \\ \left[\frac{2^n n!}{2^m m!}\right]^{1/2} \left[\frac{\hbar}{\mu\omega_c}\right]^{(m-n)/2} [iq_y - q_x \text{sgn}(e)]^{m-n} L_n^{m-n} \left[\frac{\hbar}{2\mu\omega_c}(q_x^2 + q_y^2)\right], & n \leq m. \end{cases} \tag{15}$$

In the above, $L_m^n(q)$ are the associated Laguerre polynomials.¹⁶ Substitution of these matrix elements into Eq. (7) yields the result

$$\begin{aligned} \vec{\sigma}(\mathbf{q}, \mathbf{q}', \omega) = & \frac{ie^2}{\mu L^2 \hbar} \sum_{\substack{n,m \\ k_x, k_x'}} \frac{F(m) - F(n)}{\omega - (E_n - E_m)/\hbar + i\eta} \delta_{k_x', k_x - q_x} \delta_{q_y', q_x} \mathbf{M}_1(q) \mathbf{M}_2(q') \\ & \times e^{-\hbar/m\omega_c \{ (1/4)(q_x^2 + q_y^2 + q_x'^2 + q_y'^2) + i \text{sgn}(e)[(q_y' - q_y)k_x - (1/2)(q_x' q_y' - q_x q_y)] \}} \\ & + \frac{ie^2}{\mu L^2 \omega} \sum_{\substack{n \\ k_x}} F(n) \delta_{q_y', q_x} L_n \left[\frac{\hbar(q_y' - q_y)^2}{2\mu\omega_c} \right] e^{-\hbar/m\omega_c \{ (1/4)(q_y' - q_y)^2 + \text{sgn}(e)k_x(q_y' - q_y) \}} \left[\mathbf{I} - \frac{\mathbf{q}\mathbf{q}'}{q'^2} \right], \end{aligned} \tag{16}$$

where $L_n(q)$ denotes $L_n^0(q)$. Next we perform the summations over k_x and k_x' , leading to the result

$$\vec{\sigma}(\mathbf{q}, \mathbf{q}', \omega) = \vec{\sigma}(\mathbf{q}, \omega) \delta_{\mathbf{q}, \mathbf{q}'}, \tag{17}$$

which is to be expected due to the rotational symmetry of the system, with

$$\vec{\sigma}(\mathbf{q}, \omega) = \frac{ie^2 \omega_c}{2\pi \hbar^2} e^{-\hbar/2\mu\omega_c (q_x^2 + q_y^2)} \sum_{n,m} \frac{F(m) - F(n)}{\omega - (E_n - E_m)/\hbar + i\eta} \mathbf{M}_1(q) \mathbf{M}_2(q) + \frac{ie^2 \rho}{\mu\omega} \left[\mathbf{I} - \frac{\mathbf{q}\mathbf{q}}{q^2} \right]. \tag{18}$$

In Eq. (18) we have used the result $L_n(0) = 1$, and the number density $\rho = N/L^2$ has been introduced.

For simplicity and consistency with previous work,^{7,14} we now take $q_x = 0$, and consequently $q = |\mathbf{q}|$ can be used interchangeably with q_y .

We now evaluate the four tensor components at zero temperature. The zero-temperature boson distribution function is

$$F(n) = Ng^{-1} \delta_{n,0}, \tag{19}$$

where g is the usual Landau degeneracy factor:

$$g = \frac{\mu\omega_c L^2}{2\pi \hbar}. \tag{20}$$

Introducing the distribution function (19) and the energy eigenvalues from (12), we find

$$\vec{\sigma}(\mathbf{q}, \omega) = \frac{ie^2 \rho}{\mu \hbar} e^{-(q^2/2q_B^2)} \vec{Y} + \frac{ie^2 \rho}{\mu \omega} \left[\mathbf{I} - \frac{\mathbf{q}\mathbf{q}}{q^2} \right], \quad (21)$$

$$\vec{Y} = \sum_n \frac{1}{\omega - n\omega_c + i\eta} \begin{Bmatrix} \text{sgn}(e)\hbar q_B \left[\left[\frac{n}{2} \right]^{1/2} {}^{n-1}F_0^* + \left[\frac{n+1}{2} \right]^{1/2} {}^{n+1}F_0^* \right] \\ i\hbar q_B \left[\left[\frac{n+1}{2} \right]^{1/2} {}^{n+1}F_0^* - \left[\frac{n}{2} \right]^{1/2} {}^{n-1}F_0^* \right] - \frac{\hbar}{2} q^n F_0^* \end{Bmatrix} \begin{Bmatrix} \frac{\text{sgn}(e)\hbar q_B}{} {}^n F_1 \\ \frac{\mu\omega\sqrt{2}}{q} {}^n F_0 \end{Bmatrix}$$

$$- \sum_n \frac{1}{\omega + n\omega_c + i\eta} \begin{Bmatrix} \frac{\text{sgn}(e)\hbar q_B}{} {}^n F_n^* \\ \frac{i\hbar q_B}{} {}^n F_n^* - \frac{\hbar}{2} q^n F_n^* \end{Bmatrix} \begin{Bmatrix} \frac{\text{sgn}(e)\hbar q_B}{} \left[\left[\frac{n}{2} \right]^{1/2} {}^0 F_{n-1} + \left[\frac{n+1}{2} \right]^{1/2} {}^0 F_{n+1} \right] \\ \frac{1}{q} {}^0 F_n \end{Bmatrix}.$$

We now evaluate the four components of the conductivity tensor. We employ the special cases¹⁶ of the Laguerre polynomial:

$$L_1^\alpha(x) = \alpha + 1 - x, \quad (22)$$

$$L_0^\alpha(x) = 1,$$

in order to evaluate the functions occurring in Eq. (21). The resulting components are

$$\sigma_{yy}(q, \omega) = \frac{i\rho e^2 \omega_c}{\hbar q^2} e^{-(q^2/2q_B^2)} \sum_{n=1}^{\infty} \frac{(q^2/2q_B^2)^n}{(n-1)!} \left[\frac{1}{n\omega_c + \omega + i\eta} - \frac{1}{n\omega_c - \omega - i\eta} \right],$$

$$\sigma_{xx}(q, \omega) = \frac{i\rho e^2 \omega_c^2}{2\mu\omega^2} e^{-(q^2/2q_B^2)} \sum_{n=1}^{\infty} \frac{(q^2/2q_B^2)^{n-1}}{(n-1)!} \left[n - \frac{q^2}{2q_B^2} \right]^2 \left[\frac{1}{n\omega_c + \omega + i\eta} - \frac{1}{n\omega_c - \omega - i\eta} \right] + \frac{i\rho e^2}{\mu\omega},$$

$$\sigma_{yx}(q, \omega) = \frac{\rho e^2 \text{sgn}(e) \omega_c^2}{\hbar q^2 \omega} e^{-(q^2/2q_B^2)} \sum_{n=1}^{\infty} \frac{(q^2/2q_B^2)^n}{(n-1)!} \left[n - \frac{q^2}{2q_B^2} \right] \left[\frac{1}{n\omega_c + \omega + i\eta} - \frac{1}{n\omega_c - \omega - i\eta} \right]$$

$$= -\sigma_{xy}(q, \omega). \quad (23)$$

The components displayed above can be expressed in terms of the Kummer hypergeometric functions. This will be carried out in Sec. IV.

IV. DISPERSION RELATIONS

We discuss the modes of electrodynamic oscillation for the planar boson plasma, using results from Sec. III. It can be shown^{7,14} that these oscillations are governed by the dispersion relation

$$\left[i\sigma_{xx}(q, \omega) - \frac{\beta c^2}{2\pi\omega} \right] \left[i\sigma_{yy}(q, \omega) + \frac{\omega}{2\pi\beta} \right] + \sigma_{xy}(q, \omega)\sigma_{yx}(q, \omega) = 0, \quad (24)$$

where, as in Sec. III, we have chosen the direction of propagation to be in the y direction, i.e., $q_x = 0$. In general, the conductivity tensor has both real and imaginary parts, and the solutions $\omega(q)$ of the above dispersion relation are likewise complex:

$$\omega = \omega_r + i\gamma. \quad (25)$$

The imaginary part γ of $\omega(q)$ is known as the damping constant. We now make an approximation, similar to that employed by Harris,¹³ the so-called *weak damping* approximation, in which it is assumed that the damping constant is small. In the case of the three-dimensional plasmas studied by Harris, it was also assumed that the imaginary part of the longitudinal dielectric response function is small. These assumptions allowed the dispersion relation to be separately solved for the real and imaginary parts of ω .

For the two-dimensional plasma studied here, it is necessary to assume that the quantities $\text{Re}[\sigma_{xx}(q, \omega_r)]$, $\text{Re}[\sigma_{yy}(q, \omega_r)]$, $\text{Im}[\sigma_{xy}(q, \omega_r)]$, and $\text{Im}[\sigma_{yx}(q, \omega_r)]$ are small in order to solve the more complicated dispersion relation (24) separately for ω_r and γ . These assumptions will be shown to be valid for all physical cases investigated here. If

products of small quantities are neglected, we are left with the following equation for the frequency of oscillation ω_r :

$$\left[-\text{Im}[\sigma_{xx}(q, \omega_r)] - \frac{\beta_r c^2}{2\pi\omega_r} \right] \left[-\text{Im}[\sigma_{yy}(q, \omega_r)] + \frac{\omega_r}{2\pi\beta_r} \right] + \text{Re}[\sigma_{xy}(q, \omega_r)]\text{Re}[\sigma_{yx}(q, \omega_r)] = 0. \quad (26)$$

In what follows we will always assume, without loss of generality, that $\omega_r > 0$.

If we assume that ω_r is not a multiple of the cyclotron frequency ω_c , then we can immediately take the $\eta \rightarrow 0$ limit in Eq. (23), yielding the following results for the conductivity components:

$$\begin{aligned} \text{Re}[\sigma_{yy}(q, \omega_r)] &= 0, \\ \text{Im}[\sigma_{yy}(q, \omega_r)] &= \frac{\rho e^2 \omega_c}{\hbar q^2} e^{-(q^2/2q_B^2)} \sum_{n=1}^{\infty} \frac{(q^2/2q_B^2)^n}{(n-1)!} \left[\frac{1}{n\omega_c + \omega_r} - \frac{1}{n\omega_c - \omega_r} \right], \\ \text{Re}[\sigma_{xx}(q, \omega_r)] &= 0, \\ \text{Im}[\sigma_{xx}(q, \omega_r)] &= \frac{\rho e^2}{\mu\omega_r} + \frac{\rho e^2 \omega_c^2}{2\mu\omega_r^2} e^{-(q^2/2q_B^2)} \sum_{n=1}^{\infty} \frac{(q^2/2q_B^2)^{n-1}}{(n-1)!} \left[n - \frac{q^2}{2q_B^2} \right]^2 \left[\frac{1}{n\omega_c + \omega_r} - \frac{1}{n\omega_c - \omega_r} \right], \\ \text{Re}[\sigma_{yx}(q, \omega_r)] &= \frac{\rho e^2 \text{sgn}(e)\omega_c^2}{\hbar q^2 \omega_r} e^{-(q^2/2q_B^2)} \sum_{n=1}^{\infty} \frac{(q^2/2q_B^2)^n}{(n-1)!} \left[n - \frac{q^2}{2q_B^2} \right] \left[\frac{1}{n\omega_c + \omega_r} - \frac{1}{n\omega_c - \omega_r} \right] \\ &= -\text{Re}[\sigma_{xy}(q, \omega_r)], \\ \text{Im}[\sigma_{yx}(q, \omega_r)] &= 0 \\ &= \text{Im}[\sigma_{xy}(q, \omega_r)], \end{aligned} \quad (27)$$

where we have the restriction

$$\omega_r \neq n\omega_c, \quad n = 1, 2, \dots \quad (28)$$

We now express these components in terms of Kummer hypergeometric functions $\Phi(1, 1+x, -z)$, which are defined¹⁶ as

$$\Phi(1, 1+x, -z) = x e^{-z} \sum_{n=0}^{\infty} \frac{z^n}{n!} \frac{1}{n+x}. \quad (29)$$

From this definition, the following related formulas, which we require, can be derived:

$$\begin{aligned} \sum_{n=1}^{\infty} \frac{z^n}{(n-1)!} \frac{1}{n+x} &= e^z [1 - \Phi(1, 1+x, -z)], \\ \sum_{n=1}^{\infty} \frac{z^n}{(n-1)!} \frac{n-z}{n+x} &= e^z [(z+x)\Phi(1, 1+x, -z) - x], \\ \sum_{n=1}^{\infty} \frac{z^n}{(n-1)!} \frac{(n-z)^2}{n+x} &= e^z \left\{ 1 - \left[1 + \frac{x}{z} \right] [(z+x)\Phi(1, 1+x, -z) - x] \right\}. \end{aligned} \quad (30)$$

At this point we introduce scaled variables for the frequency and wave number squared:

$$x = \frac{\omega_r}{\omega_c}, \quad z = \frac{q^2}{2q_B^2}. \quad (31)$$

The components in Eq. (27) may now be expressed in terms of Kummer functions:

$$\begin{aligned} \text{Im}[\sigma_{yy}(q, \omega_r)] &= \frac{\rho e^2}{2\hbar q_B^2} \frac{\Phi(1, 1-x, -z) - \Phi(1, 1+x, -z)}{z}, \\ \text{Im}[\sigma_{xx}(q, \omega_r)] &= \frac{\rho e^2}{2\mu\omega_c} \left\{ \frac{4}{x} + \frac{(z-x)^2 \Phi(1, 1-x, -z) - (z+x)^2 \Phi(1, 1+x, -z)}{x^2 z} \right\}, \\ \text{Re}[\sigma_{yx}(q, \omega_r)] &= \frac{\rho e^2 \text{sgn}(e)}{2\hbar q_B^2} \left\{ \frac{z+x}{xz} \Phi(1, 1+x, -z) + \frac{x-z}{xz} \Phi(1, 1-x, -z) - \frac{2}{z} \right\} \\ &= -\text{Re}[\sigma_{xy}(q, \omega_r)]. \end{aligned} \quad (32)$$

Incorporating the above expression into the dispersion relation (24), and converting to scaled variables, the dispersion relation becomes

$$\left[\frac{(z+x)^2 \Phi(1, 1+x, -z) - (z-x)^2 \Phi(1, 1-x, -z)}{x^2 z} - \frac{4}{x} - \frac{\sqrt{z-\chi x^2}}{\lambda x} \right] \times \left[\frac{\Phi(1, 1+x, -z) - \Phi(1, 1-x, -z)}{z} + \frac{\chi}{\lambda} \frac{x}{\sqrt{z-\chi x^2}} \right] - \left[\frac{z+x}{zx} \Phi(1, 1+x, -z) + \frac{x-z}{zx} \Phi(1, 1-x, -z) - \frac{2}{z} \right]^2 = 0, \quad x \neq n, \quad (33)$$

where we have introduced a dimensionless density parameter

$$\lambda = \frac{\pi \rho e^2}{\sqrt{2} q_B \mu c^2}, \quad (34)$$

and a dimensionless magnetic-field strength parameter

$$\chi = \frac{\hbar \omega_c}{2 \mu c^2}. \quad (35)$$

This form of the dispersion relation is appropriate for analytic and numerical plasmon studies at finite magnetic fields. It is apparent that when q is small and the frequency is sufficiently close to a multiple of the cyclotron frequency (i.e., $x \sim n; n = 1, 2, \dots$), the Landau summations occurring in the conductivity components (27) are dominated by the term corresponding to the resonance, in addition to the $n = 1$ term which is nonzero as $q \rightarrow 0$. The solutions $x_n(z)$ of the dispersion relation in these regions may lie extremely close to the integers, but the cyclotron resonances themselves are forbidden frequencies because the conductivity components occurring in the left-hand side of the dispersion relation are obviously infinite as $x \rightarrow n$. These modes are the quantum analogs of the so-called "Bernstein modes" or "Bernstein resonances" which were investigated for three-dimensional classical plasmas by Bernstein,¹⁷ following the work of Gross,¹⁸ who noted that certain frequency bands, spaced at intervals roughly equal to the Larmor frequency, did not support plasma oscillations in magnetized plasmas. Bernstein¹⁷ showed that modes lying close to the resonant frequencies modes are undamped. Later, the Bernstein modes were studied in detail for classical plasmas by Dougherty and Monaghan,¹⁹ Shkarofsky and Johnston,²⁰ and others. Dougherty and Watson²¹ review theoretical and experimental investigation of these modes in the context of ionospheric physics. In the case of quantum Fermi plasmas, these modes were investigated in three dimensions by Horing,²² and in two dimensions by Horing and Yildiz²³ and Chiu and Quinn.⁷ This work will be discussed in detail elsewhere,²⁴ where we make appropriate comparison with results for the Fermi plasma.

These resonances arise in more conspicuous fashion in quantum plasmas due to Landau quantization than in the classical case, where their presence is revealed by Bessel function expansions of the response functions.¹⁷

Returning to the two-dimensional Bose plasma, an analytic investigation of the solutions x_n was undertaken by

Hines,²⁵ who solved for the small quantity $x_n^2 - n^2$, neglecting all terms with $n > 1$ in the Landau summations except the resonance term. The details of these results are incorrect, however, because (as has already been noted) the tensor employed by Hines²⁵ and, earlier, Harris¹³ is incomplete due to the neglect of certain terms in the current operator (4). Later in this section we employ numerical solutions of Eq. (33) to study the three lowest Bernstein modes.

Of particular interest for numerical investigation is the possibility of solutions to the dispersion relation (33) lying below the cyclotron frequency. The existence of such solutions is investigated below, analytically and numerically, for large B in the small- q region. These modes, which can extend into the $q \rightarrow 0$ region, are qualitatively different from the higher Bernstein modes, which must terminate at the light cone at finite wave numbers.

The dispersion relation (24) was derived under the weak damping approximation. From expressions for the conductivity components (27), in particular the results $\text{Re}[\sigma_{yy}] = \text{Re}[\sigma_{xx}] = \text{Im}[\sigma_{xy}] = \text{Im}[\sigma_{yx}] = 0$, it is clear that the conditions for the validity of this approximation are satisfied. Further, it is easily shown, given the above results, that the damping constant γ is zero. Thus all solutions to the dispersion relation (24) represent undamped plasma modes. We note that similar results were found by Horing²² in the case of magnetized Fermi plasmas. This result is not surprising in the Bose case, where in the $B \rightarrow 0$ limit we must recover the undamped principal plasma mode. In the Fermi case, however, the $B = 0$ plasma mode is damped. Careful investigation of the $B \rightarrow 0$ limit, involving so-called "phase mixing" evaluation²² (essentially passing Landau sums to integrals), is required to show the reduction of an infinite number of undamped modes into a single damped mode.

A. Small- B limit

We now consider the small- B limit of the dispersion relation (26). Although the restriction $x \neq n$ associated with the above dispersion relation does not affect its utility for finite B (since the resonances are forbidden frequencies), the situation is not as simple in the small- B limit, where x becomes large and the spacing between the Landau levels becomes vanishingly small. We use the identities appearing in Eq. (30) and the conductivity components (23) to rewrite the dispersion relation while postponing the $\eta \rightarrow 0$ limit:

$$\lim_{\eta \rightarrow 0} \left\{ \left[\frac{\Phi(1, 1+x+i\eta, -z) - \Phi(1, 1-x-i\eta, -z)}{z} + \frac{\chi}{\lambda} \frac{x}{\sqrt{z-\chi x^2}} \right] \right. \\ \times \left[\frac{(z+x+i\eta)^2 \Phi(1, 1+x+i\eta, -z) - (z-x-i\eta)^2 \Phi(1, 1-x-i\eta, -z)}{x^2 z} - \frac{4}{x} - \frac{\sqrt{z-\chi x^2}}{\lambda x} \right] \\ \left. - \left[\frac{z+x+i\eta}{zx} \Phi(1, 1+x+i\eta, -z) - \frac{z-x-i\eta}{zx} \Phi(1, 1-x-i\eta, -z) - \frac{2}{z} \right]^2 \right\} = 0. \quad (36)$$

In order to find the $B \rightarrow 0$ limit we require a large z , large x expansion of the Kummer functions appearing in (36). Making use of the following little known results (see Appendix B for details):

$$\lim_{\eta \rightarrow 0} x^{-1} \Phi(1, 1+x+i\eta, -z) \\ = \frac{1}{(x+z)} + \frac{z}{(x+z)^3} - \frac{z}{(x+z)^4} + \frac{3z^2}{(x+z)^5} + \dots, \quad (37)$$

where $|x+z| \neq 0$, and

$$\lim_{\eta \rightarrow 0} x^{-1} \Phi(1, 1-x-i\eta, -z) \\ = \frac{1}{(x-z)} + \frac{z}{(x-z)^3} + \frac{z}{(x-z)^4} + \frac{3z^2}{(x-z)^5} + \dots, \quad (38)$$

where $|x-z| \neq 0$, we evaluate the dispersion relation (33) for large z and large x , subject to the conditions above, which represent the singularities of the small- B dispersion relation. For the expansion to be useful requires $|x+z| \gg 1$ and $|x-z| \gg 1$. Since we have assumed $x > 0$ and $z > 0$, it is sufficient to investigate the latter. We would not expect this condition to be violated because the relation $x=z$ corresponds to $\omega = \bar{q}/2$ which is a lower bound for the zero B dispersion relation.¹⁴ The consistency of this condition with the dispersion relations obtained using the above expansions is discussed later in this section for the various regions of interest.

As expected, we find that the cross terms σ_{xy} and σ_{yx} vanish in the $B \rightarrow 0$ limit, and the dispersion relation decouples into longitudinal and transverse branches:

$$(\bar{\rho} + \sqrt{\bar{q}^2 - \bar{\omega}^2}) \left[\frac{1}{\bar{\rho} \sqrt{\bar{q}^2 - \bar{\omega}^2}} + \frac{1}{\bar{q}^4/4 - \bar{\omega}^2} \right] = 0, \quad (39)$$

where we have introduced scaled variables more appropriate for the $B \rightarrow 0$ limit:

$$\bar{q} = \frac{\hbar q}{\mu c}, \\ \bar{\omega} = \frac{\hbar \omega}{\mu c^2}, \\ \bar{\rho} = \frac{2\pi \hbar \rho e^2}{\mu^2 c^3}. \quad (40)$$

The longitudinal branch is easily solved for the plasmon modes:

$$\bar{\omega}(\bar{q}) = \left[\frac{\bar{q}^4}{4} + \frac{\bar{\rho}^2}{2} \left[1 + \frac{\bar{q}^2}{\bar{\rho}^2} (4 - \bar{q}^2) \right]^{1/2} - \frac{\bar{\rho}^2}{2} \right]^{1/2}. \quad (41)$$

This result for the zero B longitudinal modes was obtained by Hines,²⁵ and is in agreement with the results of Hines and Frankel,¹² but only in the nonretarded region where $\beta \sim q$. The dispersion relation (41), on the other hand, is valid for all values of q .

The transverse branch clearly has no real solutions. The absence of transverse modes is a feature of the extreme physical constraint of the system (i.e., its anisotropic geometry).

We now examine the coupled plasmon modes satisfying (33) for small B fields. The frequency is expanded for small B as follows:

$$\bar{\omega} = c_0 + c_1 \left[\frac{|e| \hbar B}{\mu^2 c^3} \right] + c_2 \left[\frac{e^2 \hbar^2 B^2}{\mu^4 c^6} \right] + \dots \quad (42)$$

Substituting the expansion into (33), and once again employing the large argument expansion (37) for the Kummer functions, the dispersion relation is reduced to the form

$$(\bar{\rho} + \sqrt{\bar{q}^2 - c_0^2}) \left[\frac{1}{\bar{\rho} \sqrt{\bar{q}^2 - c_0^2}} + \frac{1}{\bar{q}^4/4 - c_0^2} \right] + [f_1(\bar{q}, \bar{\rho}, c_0) + c_1 g_1(\bar{q}, \bar{\rho}, c_0)] \left[\frac{|e| \hbar B}{\mu^2 c^3} \right] \\ + [f_2(\bar{q}, \bar{\rho}, c_0, c_1) + c_2 g_2(\bar{q}, \bar{\rho}, c_0, c_1)] \left[\frac{e^2 \hbar^2 B^2}{\mu^4 c^6} \right] + O \left[\frac{|e|^3 \hbar^3 B^3}{\mu^6 c^9} \right] = 0. \quad (43)$$

Solving for the coefficients, the equation for c_0 is of course precisely the $B=0$ dispersion relation (39), with the solution appearing in Eq. (41). The remaining coefficients are of the form

$$c_1 = -\frac{f_1(\bar{q}, \bar{\rho}, c_0)}{g_1(\bar{q}, \bar{\rho}, c_0)},$$

$$c_2 = -\frac{f_2(\bar{q}, \bar{\rho}, c_0, c_1)}{g_2(\bar{q}, \bar{\rho}, c_0, c_1)},$$
(44)

with

$$f_1(\bar{q}, \bar{\rho}, c_0) = \frac{\bar{q}^2 \left[3c_0^2 \bar{q}^2 - 4c_0^4 + \frac{c_0^2 \bar{q}^4}{4} + \frac{\bar{q}^6}{4} - \frac{\bar{q}^8}{16} + 4\rho c_0^2 \sqrt{\bar{q}^2 - c_0^2} \right]}{2 \left[\frac{\bar{q}^4}{4} - c_0^2 \right]^3 \sqrt{\bar{q}^2 - c_0^2}},$$

$$g_1(\bar{q}, \bar{\rho}, c_0) = \frac{c_0 \left[2c_0^4 - 3c_0^2 \bar{q}^2 + 2\bar{q}^4 - \frac{c_0^2 \bar{q}^4}{4} - \frac{\bar{q}^6}{4} + \frac{\bar{q}^8}{16} + 2\bar{\rho}(\bar{q}^2 - c_0^2)^{3/2} \right]}{\left[\frac{\bar{q}^4}{4} - c_0^2 \right]^2 (\bar{q}^2 - c_0^2)^{3/2}}.$$
(45)

We have omitted details of the functions $f_2(\bar{q}, \bar{\rho}, c_0, c_1)$ and $g_2(\bar{q}, \bar{\rho}, c_0, c_1)$ for the sake of brevity, due to their cumbersome algebraic form. The full expressions are readily obtained using the method above, at the expense of some tedious calculation. It is easily shown that the wave number and density structure of the leading magnetic-field correction to the plasmon frequency (i.e., c_1) is determined only by the longitudinal part of the dispersion relation. The next term (i.e., c_2) is determined by the entire coupled dispersion relation. Thus the plasmons are no longer totally longitudinal at order B^2 and above. In interpreting expansion (42) we stress that the magnetic-field strength is assumed to be small with respect to the density and wave-number parameters. Thus although the coefficients c_1 and c_2 are exact for all \bar{q} and $\bar{\rho}$, their application at small values of these parameters is valid only for correspondingly small magnetic fields. In the following, we use expansions of the functions $f_1(\bar{q}, \bar{\rho}, c_0)$ and $g_1(\bar{q}, \bar{\rho}, c_0)$ for small \bar{q} . The form of the resulting expansions for $\bar{\omega}$ clearly reflects the above-mentioned requirements. In addition, the self-consistency of the dispersion relations with the asymptotic expansions (37) used to derive them is examined in the various regions.

1. Small- \bar{q} limit; $\bar{q} \ll 1, \bar{\rho} \gg \bar{q}$.

Expanding the above coefficients for small \bar{q} leads to the result

$$\bar{\omega} = \left[\bar{q} - \frac{1}{2\bar{\rho}^2} \bar{q}^3 + O(\bar{q}^5) \right] + \left[\frac{3\bar{q}^3}{2\bar{\rho}^2} + O(\bar{q}^5) \right] \left[\frac{|e|\hbar B}{\mu^2 c^3} \right] + O \left[\frac{e^2 \hbar^2 B^2}{\mu^4 c^6} \right].$$
(46)

This expansion is good provided \bar{q} and $\bar{q}/\bar{\rho}$ are small. In addition, the requirement $|x - z| \gg 1$ yields the condition

$$\bar{q} \gg \frac{|e|\hbar B}{\mu^2 c^3}$$
(47)

for consistency of this solution with the small- B expansion. The leading (light cone) term indicates that in this region retardation effects due to the anisotropy of the system are dominating the physics. This leading term is the same as that obtained by Stern⁶ for the electron gas.

2. Small- \bar{q} limit; $\bar{q} \ll 1, \bar{\rho} \ll \bar{q}$.

As \bar{q} increases toward $\bar{\rho}$, the previous small- \bar{q} expansion becomes invalid. For $\bar{q} \gg \bar{\rho}$ the following small- \bar{q} , small- $\bar{\rho}/\bar{q}$ expansion is obtained:

$$\bar{\omega} = \left[\bar{q}\bar{\rho} + \frac{\bar{q}^4}{4} - \frac{\bar{q}^3\bar{\rho}}{8} + \frac{\bar{\rho}^3}{8\bar{q}} + O(\bar{q}\bar{\rho}^3, \bar{q}^5\bar{\rho}) \right]^{1/2} + [\gamma(\bar{q}, \bar{\rho}) + \dots] \left[\frac{|e|\hbar B}{\mu^2 c^3} \right] + O \left[\frac{e^2 \hbar^2 B^2}{\mu^4 c^6} \right],$$
(48)

where $\gamma(\bar{q}, \bar{\rho})$ denotes leading term in the small- \bar{q} , small- $\bar{\rho}/\bar{q}$ expansion of c_1 . Provided $[\bar{q} < (4\bar{\rho})^{1/3}]$, the $\bar{q}\bar{\rho}$ term in (48) dominates, leading to the asymptotic form

$$\bar{\omega} \sim \sqrt{\bar{q}\bar{\rho}}$$
(49)

for the plasmon modes. The form (49) is in agreement with the results of Stern,⁶ who first derived the analogous result for the planar Fermi plasma at $T=0$. The leading magnetic-field correction to the plasmon dispersion relation for this region is

$$\gamma(\bar{q}, \bar{\rho}) \frac{|e|\hbar B}{\mu^2 c^3} = -\frac{3\bar{q}}{4} \left[\frac{\bar{q}}{\bar{\rho}} \right]^{1/2} \frac{|e|\hbar B}{\mu^2 c^3}.$$
(50)

This result is consistent with the small- B expansion when

$$\bar{\rho}\bar{q} \gg \frac{e^2 \hbar^2 B^2}{\mu^4 c^6}.$$
(51)

If \bar{q} increases still further $[\bar{q} > (4\bar{\rho})^{1/3}]$, the \bar{q}^4 term in (48) will dominate, yielding the dispersion relation

$$\bar{\omega} \sim \frac{\bar{q}^2}{2}.$$
(52)

This result contrasts with the $\omega \sim v_f q$ dependence observed by Stern⁶ and Fetter⁸ in the corresponding region for the Fermi plasma, where v_f is the Fermi velocity. The leading magnetic-field correction term in this region is

$$\gamma(\bar{q}, \bar{\rho}) \frac{|e| \hbar B}{\mu^2 c^3} = \frac{\bar{q}^3 |e| \hbar B}{2 \bar{\rho} \mu^2 c^3}. \quad (53)$$

In this region, the dispersion relation is consistent with the small- B expansion for

$$\frac{\bar{\rho}}{\bar{q}} \gg \frac{|e| \hbar B}{\mu^2 c^3} \quad (54)$$

B. Large B

We now investigate the plasma oscillations for large, laboratory scale (as opposed to astrophysical) field strengths. We use the dispersion relation (33) as a starting point for analytical and numerical investigation. The cyclotron resonances in the magnetized plasma fundamentally alter the nature of the dispersion relation in comparison with the unmagnetized plasma. In the unmagnetized case a single, continuous plasmon mode occurs, while in the magnetized plasma an infinite number of separate modes occur, each of which is restricted to a finite range of frequencies, scales by ω_c .

The plasmon dispersion relation (33) does not have purely longitudinal nor purely transverse solutions. We show that the proximity of the plasmon mode to the light cone, as measured by $\beta = \sqrt{z - \omega^2/c^2}$, determines the physical nature of the plasmons. For solutions very close to the light cone, β approaches zero. In the scaled variables of Eq. (33), this means that $\sqrt{z - \chi x^2}$ is very small. For the purposes of this discussion we rewrite (33) in the shorthand form

$$\left[t_{xx} - \frac{\sqrt{z - \chi x^2}}{\lambda x} \right] \left[t_{yy} + \frac{\chi x}{\lambda \sqrt{z - \chi x^2}} \right] - t_{yx}^2 = 0, \quad (55)$$

where the tensor \vec{t} has components

$$\begin{aligned} t_{yy} &= -\text{Im}[\sigma_{xx}] \frac{2\mu\omega_c}{\bar{\rho}e^2}, \\ t_{xx} &= -\text{Im}[\sigma_{yy}] \frac{2\mu\omega_c}{\bar{\rho}e^2}, \\ t_{yx} &= \text{Re}[\sigma_{yx}] \frac{2\mu\omega_c}{\bar{\rho}e^2 \text{sgn}(e)}. \end{aligned} \quad (56)$$

These components are written in terms of Kummer functions [see Eqs. (32)] and contain poles at $x = 1, 2, 3, \dots$. The dispersion relation Eq. (55) can be viewed as the product of “transverse” and “longitudinal” branches with the addition of a coupling term (i.e., $-t_{yx}^2$). In what follows, frequent reference is made to solutions of longitudinal and transverse “branches” of the dispersion relation. When such solutions are substituted into the fully coupled dispersion relation, the left-hand side of Eq. (55) is reduced to the coupling term $-t_{yx}^2$. The magnitude of this term then determines the physical relevance of the

“longitudinal” or “transverse” solutions.

If the coupling term is large then these solutions do not even approximately solve the full dispersion relation and are physically meaningless. In such strongly coupled regions the transverse and longitudinal components of the electric field associated with the plasmons will both be significant.

If the coupling term is very small then these solutions are physically meaningful as approximations to the full solutions of the coupled dispersion relation. In such weakly coupled regions the plasmon electric field will be almost longitudinal (or transverse), but will nevertheless contain a **small transverse** (or longitudinal) component.

When $\sqrt{z - \chi x^2}$ approaches zero, the “longitudinal” branch cannot have solutions except where t_{yy} is large, i.e., very near the singularities of the Kummer function. In this region, however, the coupling term t_{yx}^2 will also be large, so solutions of the “longitudinal” branch would not be expected to satisfy the full dispersion relation (55), and would be physically meaningless. On the other hand, the “transverse” branch

$$t_{xx} - \frac{\sqrt{z - \chi x^2}}{\lambda x} = 0 \quad (57)$$

will have zeros when t_{xx} is positive and not too near to the singularities, where it might be anticipated that the coupling term t_{yx}^2 would be negligible. In regions where this is the case, the solutions of the “transverse” branch closely approximate the solutions of the full coupled dispersion relation and are therefore physically meaningful. We now investigate such “nearly transverse” modes in detail.

We want to look for solutions near the light cone for a range of x values including the first few Bernstein resonances. For definiteness, let us consider the n th Bernstein mode, i.e., $x \sim n$. For modes in the vicinity of the light cone, we have $x \sim (\bar{q}/2\chi)$, which means, in view of the previous result, that $\bar{q} \sim 2n\chi$ or less. Even for extremely large laboratory scale fields, the parameter χ is still very small. For example, a magnetic-field strength of 10^7 G corresponds to $\chi = 1.1 \times 10^{-7}$. So provided n is not too large, $\bar{q} \ll 1$ and therefore the parameter z (i.e., $\bar{q}^2/4\chi$) is very small. We can therefore neglect all but the first term in the Landau series for t_{xx} , provided x is not too close to an integer n where $n > 1$, yielding

$$t_{xx} \sim -\frac{2}{x} + \frac{2}{x} e^{-z} \frac{(1-z)^2}{1-x^2}. \quad (58)$$

Now neglecting all corrections of order z or higher in the above, we write the transverse branch (57) as

$$\frac{2x}{1-x^2} - \frac{\sqrt{z - \chi x^2}}{\lambda x} = 0. \quad (59)$$

We first note that this equation has no real solutions when $x > 1$. With this in mind we rewrite (59) as a cubic in x^2 :

$$x^6 + x^4 \left[4 \frac{\lambda^2}{\chi} - \frac{z}{\chi} - 2 \right] + x^2 \left[1 + \frac{2z}{\chi} \right] - \frac{z}{\chi} = 0. \quad (60)$$

In the region below the light cone [i.e., $x < \bar{q}/2\chi$] this cubic has a positive real solution and a complex conjugate pair of solutions. The real solution, although complicated, is easily evaluated numerically. In Fig. 1 we compare this solution with a numerical solution of the full coupled dispersion relation for a particular density ($\bar{\rho}=10^{-10}$) and magnetic field ($\chi=5\times 10^{-7}$).

Clearly the transverse branch provides an excellent approximation of the exact solution for plasmon frequencies from zero up until very close to resonance (in the particular case studied, the approximation is good up to approximately $x=0.9998$). Above this frequency the solution of the cubic, which must remain below $x=1$, departs drastically from the exact solution, which crosses over the resonance at ω_c . The departure of the exact solution from the transverse branch near $x=1$ indicates that the transverse-longitudinal coupling is very strong in this region, and must be included in the dispersion relation to obtain the correct behavior (i.e., the crossover at $x=1$). The onset of strong coupling coincides with the deviation of the transverse branch from the light cone, which occurs because as x approaches the singularity in t_{xx} at $x=1$, a corresponding increase in β must occur in order to cancel this contribution. The existence of essentially transverse plasmons over a large frequency range is an interesting result which is due entirely to the external magnetic field, since it has been shown¹⁴ that no transverse plasmons exist in the $B=0$ Bose plasma.

We now consider the possibility of approximately transverse modes for $x > 1$. Since the contribution from the first term in the Landau sum for t_{xx} is negative in this region, and $t_{xx} > 0$ is required to solve the transverse branch, the only possibility is that the plasmon frequency must be close to one of the higher resonances. This is consistent with the termination of the higher Bernstein modes (i.e., $n=2,3,\dots$) at the light cone: as they approach the light cone in the small- q region, $\beta \rightarrow 0$ and consequently the plasmons become increasingly transverse. Near each resonance at $x=n$, t_{xx} can be approxi-

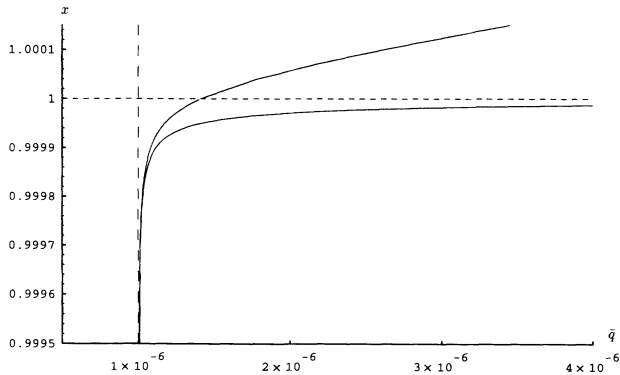


FIG. 1. Comparison of a solution of the exact coupled dispersion relation (upper curve) with a solution of the transverse branch alone (lower curve). The almost vertical dashed line is the light cone $\omega=cq$ (or $x=\bar{q}/2\chi$ in scaled variables). The density and magnetic-field parameters are $\bar{\rho}=10^{-10}$ and $\chi=5\times 10^{-7}$, respectively.

mated by taking only the resonance term and the $n=1$ term in the Landau series (27):

$$t_{xx} \sim -\frac{2}{x} + \frac{2}{x} e^{-z} \left[\frac{(1-z)^2}{1-x^2} + \frac{z^{n-1}}{(n-1)!} \frac{(n-z)^2}{n^2-x^2} \right]. \quad (61)$$

For $t_{xx} > 0$ the difference n^2-x^2 must be positive and extremely small (i.e., of order z^{n-1}). Neglecting small quantities in the above expression for t_{xx} , the transverse dispersion relation reduces to

$$\frac{2x}{1-x^2} + \frac{2n^2}{x} \frac{z^{n-1}}{(n-1)!(n^2-x^2)} = \frac{\sqrt{z-\chi x^2}}{\lambda x}. \quad (62)$$

To obtain the low-frequency cutoff for solutions, corresponding to $\beta=0$, we put $z=\chi x^2$ and set $x=n$ in the left-hand side of Eq. (62), where this is a very good approximation (i.e., everywhere except in the difference n^2-x^2) leading to the result

$$x_n^{\min} = n \left[1 - \frac{(n^2-1)(\chi n^2)^{n-1}}{n^2(n-1)!} \right]^{1/2}. \quad (63)$$

The existence of a cutoff at the light cone for the $n > 1$ Bernstein modes (in contrast to the $n=1$ mode which extends down to $x=0$) indicates that they will deviate much more rapidly from the light cone. Indeed the vicinity of $x \sim n$ is precisely where the coupling would be expected to be strong. We will see later that the $n > 1$ Bernstein modes lie above the resonances at larger wave numbers (i.e., they must cross over the resonances), so the dispersion relations will rapidly diverge from the solutions of the transverse branch, which cannot cross over $x=n$.

We now return to the plasmon mode which originates below $x=1$, where it is essentially transverse, and crosses over the resonance as the coupling becomes important. This mode is investigated in the $x > 1$ region over a large range of wave numbers. We compare the numerical solution of the full coupled dispersion relation with a similar solution of the longitudinal branch alone. First, however, we note that Hines²⁵ has shown that if the effects of both coupling and retardation are neglected, the longitudinal branch yields solutions near the cyclotron resonances, of the form

$$x^2 = n^2 + \frac{\bar{\rho}\bar{q}}{4\chi^2} z^{n-1} \quad (64)$$

to leading order in z , where $n=1,2,3,\dots$ labels the Bernstein resonances. These solutions are obtained immediately from the longitudinal branch

$$t_{yy} + \frac{\chi x}{\lambda \sqrt{z-\chi x^2}} \quad (65)$$

by making the substitution $\sqrt{z-\chi x^2} \rightarrow z$ and retaining only the resonance terms in the Landau series for t_{yy} [see Eq. (27)].

In Fig. 2 the continuation of the fully coupled solution shown in Fig. 1 into the region above $x=1$ is plotted, along with a solution of the longitudinal branch alone (without neglecting retardation) and also the $n=1$ case of the nonretarded solution given in Eq. (64).

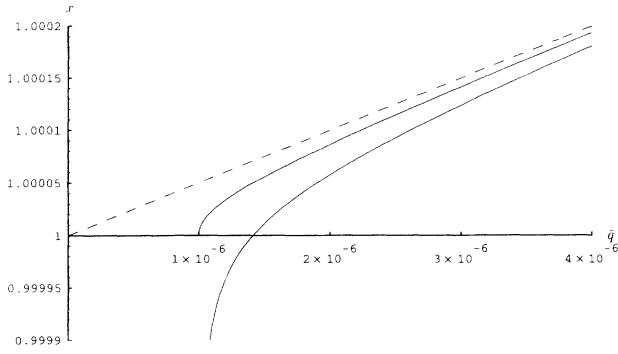


FIG. 2. Numerical solution of the fully coupled dispersion relation (lower curve) is plotted against a numerical solution of the longitudinal branch alone (center curve), and also the nonretarded solution $x^2 = 1 + (\bar{\rho}q/4\chi^2)$ (dashed line). The density and field strength parameters are the same as those used in Fig. 1.

It is interesting to note that solutions to the longitudinal branch do not exist below $x = 1$, while solutions to the transverse branch, discussed earlier, are restricted to the region $x < 1$. Clearly the effects of both retardation and coupling must be included to produce the correct plasmon behavior as a function of \bar{q} . The fully coupled solution differs substantially from the solutions of the longitudinal branch alone over a range of wave numbers which covers approximately an order of magnitude in \bar{q} from the crossover point.

As the wave number increases further, the solution of the longitudinal branch closely approximates the exact dispersion curve, indicating that the dispersion relation becomes more longitudinal in nature. This is consistent with the role played by the proximity of the light cone in determining the strength of the transverse-longitudinal coupling. As the plasmon mode moves further from the light cone, β becomes large and, as a result of the structure of the dispersion relation, the longitudinal branch becomes dominant. In Fig. 3 we plot numerical solutions

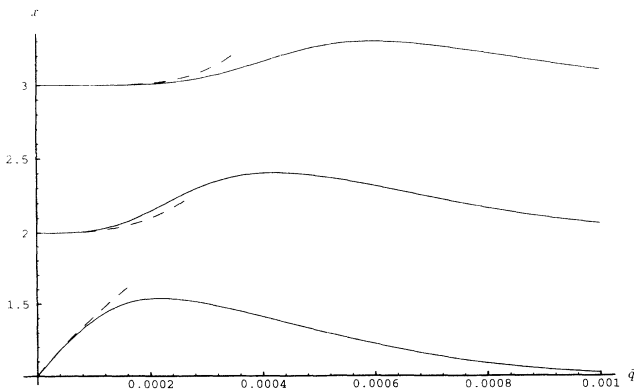


FIG. 3. Exact solutions of the dispersion relation plotted against the leading order longitudinal nonretarded approximations (dashed curves) given in Eq. (64). The field strength parameter has the value $\chi = 5 \times 10^{-8}$, which differs from those used for Figs. 1 and 2. The density parameter is $\bar{\rho} = 10^{-10}$, as in previous figures.

of the complete dispersion relation (33) over a large wave-number range for the first three Bernstein modes, and compare the results with the approximate forms given in Eq. (64).

The most striking feature of these results is the large frequency gaps in which no mode propagation can occur. This emphasizes the discrete nature of the plasmon modes in the magnetized plasma, in contrast to the zero- B case where no gaps occur in the spectrum. The nonretarded solutions (64) of the longitudinal branch describe the modes accurately while z is small (though large enough to neglect coupling), but it is necessary to take a large number of terms in the Landau summations in order to adequately describe the structure of the dispersion curves at higher wave numbers.

The dispersion relation has been studied here at zero temperature. In previous finite-temperature studies of the unmagnetized Bose plasma,¹² it was shown that the $T=0$ result is the correct leading term in the low-temperature expansion, and that small finite temperature corrections to the $T=0$ result occur only at high order in the wave-number expansion. Furthermore the two-dimensional charged Bose gas does not exhibit a finite critical temperature (with or without an applied magnetic field), so no condensation effects are being overlooked by studying the plasma strictly at $T=0$. These considerations lead us to conclude that our zero-temperature treatment provides a reasonable first approximation of the low-temperature Bose plasma, despite the fact that $T=0$ is a singular point in the Bose distribution function. A complete study of the low-temperature expansion of the plasmon modes, involving considerably greater mathematical intricacy than the present study, would nonetheless be an interesting generalization of this work.

ACKNOWLEDGMENTS

We are grateful for valuable discussions with Victor Kowalenko.

APPENDIX A: MATRIX ELEMENTS

Here we calculate the matrix elements (13) required to evaluate the conductivity tensor (7) for nonzero magnetic field. The calculation is similar to that employed by Hore and Frankel²⁶ in their study of three-dimensional Bose plasmas.

The wave functions $\psi_p(\mathbf{r}) \equiv \psi_{n,k_x}$ and $\psi_p(\mathbf{r}) \equiv \psi_{m,k'_x}$ are defined in Eq. (10). We also use the symbols q_B , ω_c , and y_0 , which are defined in Eq. (11). The basic matrix element to be considered is

$$\langle \mathbf{p} | e^{i\mathbf{q}\cdot\mathbf{r}} | \mathbf{p}' \rangle = N_n N_m I_x I_y, \quad (\text{A1})$$

with

$$I_x = \int_{-L/2}^{L/2} dx e^{i(k_x - k'_x + q_x)x}, \quad (\text{A2})$$

$$I_y = \int_{-\infty}^{\infty} dy e^{-(q_B^2/2)(y+y_0)^2} e^{-(q_B^2/2)(y+y'_0)^2} \times H_n[q_B(y+y_0)] H_m[q_B(y+y'_0)] e^{iq_y y},$$

where H_n and H_m are Hermite polynomials, and the $L \rightarrow \infty$ limit has been taken in the case of I_y . Now, due to the imposition of periodic boundary conditions, we have

$$I_x = L \delta_{k_x, k'_x + q_x}, \quad (\text{A3})$$

so that the evaluation of the integral I_y is the core of the problem. Integrals of this form do not appear in standard tables,^{16,27,28} but have been studied by Walters and Harris²⁹ and Delsante and Frankel.³⁰ Making use of results from the latter, we find

$$I_y = e^{-\left(\frac{q_B^2}{2}\right)[y_0^2 + y_0'^2 - (1/2)A^2]} \begin{pmatrix} 2^n \left[\frac{\pi}{q_B^2} \right]^{1/2} m! b^{n-m} L_m^{n-m}(-2ab) & m \leq n \\ 2^m \left[\frac{\pi}{q_B^2} \right]^{1/2} n! a^{m-n} L_n^{m-n}(-2ab) & n \leq m \end{pmatrix}, \quad (\text{A4})$$

where L_n^m is the associated Laguerre polynomial, and we have defined

$$\begin{aligned} A &= y_0 + y_0' - i \frac{q_y}{q_B}, \\ a &= \frac{q_B}{2} \left[y_0' - y_0 + i \frac{q_y}{q_B} \right], \\ b &= \frac{q_B}{2} \left[y_0 - y_0' + i \frac{q_y}{q_B} \right]. \end{aligned} \quad (\text{A5})$$

After some algebra, the above result for the matrix element is

$$\langle \mathbf{p} | e^{i\mathbf{q}' \cdot \mathbf{r}} | \mathbf{p}' \rangle = \delta_{k'_x, k_x - q_x} e^{-\left(\frac{\hbar}{\mu\omega_c}\right)\left\{\frac{1}{4}(q_x'^2 + q_y'^2) + i \operatorname{sgn}(e)[q_y' k_x - (1/2)q_x' q_y']\right\}} {}^n F_m(q'), \quad (\text{A6})$$

where ${}^n F_m(q)$ has been defined in Eq. (15).

In order to construct the matrix elements appearing in Sec. III, the following type of matrix element is required in addition to the above result:

$$\langle \mathbf{p} | e^{i\mathbf{q}' \cdot \mathbf{r}} \left[\mathbf{p} - \frac{e}{c} \mathbf{A} \right] | \mathbf{p}' \rangle = \langle n, k_x | e^{-i\mathbf{q}' \cdot \mathbf{r}} \begin{pmatrix} \frac{\hbar}{i} \frac{\partial}{\partial x} + \frac{eBy}{c} \\ \frac{\hbar}{i} \frac{\partial}{\partial y} \end{pmatrix} | m, k'_x \rangle. \quad (\text{A7})$$

For the x component, we require the result

$$\begin{aligned} \left[\frac{\hbar}{i} \frac{\partial}{\partial x} + \frac{eBy}{c} \right] \psi_{m, k'_x} &= \left[\hbar k'_x + \frac{eBy}{c} \right] \psi_{m, k'_x} \\ &= \frac{eB}{c} (y_0' + y_0) \psi_{m, k'_x} \\ &= \frac{m}{2q_B} \frac{N_m}{N_{m-1}} \psi_{m-1, k'_x} + \frac{1}{2q_B} \frac{N_m}{N_{m+1}} \psi_{m+1, k'_x}, \end{aligned} \quad (\text{A8})$$

where we have employed the recursion relation¹⁶

$$H_n(x) = 2xH_{n-1}(x) - 2(n-1)H_{n-2}(x). \quad (\text{A9})$$

The y component can be rewritten using the result

$$\frac{\partial}{\partial y} \psi_{m, k'_x} = q_B \left[\left[\frac{m}{2} \right]^{1/2} \psi_{m-1, k'_x} - \left[\frac{(m+1)}{2} \right]^{1/2} \psi_{m+1, k'_x} \right], \quad (\text{A10})$$

where, in addition to the recursion relation above, we have used¹⁶

$$\frac{\partial}{\partial x} H_n(x) = 2nH_{n-1}(x). \quad (\text{A11})$$

Combining these results with the matrix element (A6), we have

$$\langle \mathbf{p} | e^{i\mathbf{q}\cdot\mathbf{r}} \left[\mathbf{p} - \frac{e}{c} \mathbf{A} \right] | \mathbf{p}' \rangle = \delta_{k'_x, k_x - q_x} e^{-i(\hbar/\mu\omega_c)\{(1/4)(q_x^2 + q_y^2) + \text{sgn}(e)[q_y k_x - (1/2)q_x q_y]\}} \times \left[\begin{aligned} & \text{sgn}(e) \left[\frac{\hbar m \omega_c}{2} \right]^{1/2} [\sqrt{m} {}^n F_{m-1} + \sqrt{m+1} {}^n F_{m+1}] \\ & i \left[\frac{\hbar \mu \omega_c}{2} \right]^{1/2} [\sqrt{m+1} {}^n F_{m+1} - \sqrt{m} {}^n F_{m-1}] \end{aligned} \right]. \tag{A12}$$

**APPENDIX B:
ASYMPTOTIC EXPANSION OF $\Phi(1, 1+x, -z)$**

In Sec. IV we make use of asymptotic expansion for large x and large z of the Kummer functions $\Phi(1, 1+x+i\eta, -z)$ and $\Phi(1, 1-x-i\eta, -z)$, where both x and z are real and positive.

These expansions do not appear in any of the standard references on confluent hypergeometrics.^{16,27,28,31} Interestingly, they are in fact special cases of a more general result obtained by a technique of Ramanujan.³² Here we give a more accessible derivation. Using the definition of the Kummer function:¹⁶

$$\Phi(1, 1+x+i\eta, -z) = x e^{-z} \sum_{n=0}^{\infty} \frac{z^n}{n!} \frac{1}{n+x+i\eta}, \tag{B1}$$

and the result

$$\frac{1}{x+i\eta+n} = \int_0^{\infty} dt e^{-(n+x+i\eta)t}, \quad x > 0, \tag{B2}$$

we obtain the integral representation

$$\Phi(1, 1+x+i\eta, -z) = x \int_0^{\infty} dt e^{-(x+i\eta)t - z(1-e^{-t})}. \tag{B3}$$

It is readily apparent that this is an integral of the Laplace form.³³ Using Watson's lemma,³³ it is straightforward to recover the expansion

$$\begin{aligned} \Phi(1, 1+x+i\eta, -z) &= \frac{x+i\eta}{(x+i\eta+z)} + \frac{(x+i\eta)z}{(x+i\eta+z)^3} \\ &\quad - \frac{(x+i\eta)z}{(x+i\eta+z)^4} + \frac{3(x+i\eta)z^2}{(x+i\eta+z)^5} + \dots \end{aligned} \tag{B4}$$

Now, provided $|x+z| > 0$ (which has been assumed initially), we can obtain the $\eta \rightarrow 0$ limit of the above result:

$$\begin{aligned} \lim_{\eta \rightarrow 0} \Phi(1, 1+x+i\eta, -z) &= \frac{x}{(x+z)} + \frac{xz}{(x+z)^3} - \frac{xz}{(x+z)^4} + \frac{3xz^2}{(x+z)^5} + \dots \end{aligned} \tag{B5}$$

This expansion is rapidly convergent for $x, z \gg 1$, but is actually valid for $x \gg 1$, any z . Now for the expansion of $\Phi(1, 1-x-i\eta, -z)$, where by definition

$$\Phi(1, 1-x-i\eta, -z) = -x e^{-z} \sum_{n=0}^{\infty} \frac{z^n}{n!} \frac{1}{n-x-i\eta}, \tag{B6}$$

we use a slightly different integral representation,

$$\frac{1}{n-x-i\eta} = i \int_0^{\infty} dt e^{-[i(n-x)+\eta]t}, \tag{B7}$$

to obtain

$$\Phi(1, 1-x-i\eta, -z) = -ix \int_0^{\infty} dt e^{-(\eta-ix)t - z(1-e^{-it})}. \tag{B8}$$

Applying Watson's lemma again yields the expansion

$$\begin{aligned} \Phi(1, 1-x-i\eta, -z) &= \frac{x+i\eta}{(x+i\eta-z)} + \frac{(x+i\eta)z}{(x+i\eta-z)^3} \\ &\quad + \frac{(x+i\eta)z}{(x+i\eta-z)^4} + \frac{3(x+i\eta)z^2}{(x+i\eta-z)^5} + \dots \end{aligned} \tag{B9}$$

Now we take the $\eta \rightarrow 0$ limit, subject to the condition (not assumed initially) $|x-z| > 0$, with the result

$$\begin{aligned} \lim_{\eta \rightarrow 0} \Phi(1, 1-x-i\eta, -z) &= \frac{x}{(x-z)} + \frac{xz}{(x-z)^3} + \frac{xz}{(x-z)^4} + \frac{3xz^2}{(x-z)^5} + \dots \end{aligned} \tag{B10}$$

With our initial choice that $x > 0$, the $\eta \rightarrow 0$ limit is superfluous in the case of $\Phi(1, 1+x+i\eta, z)$, but necessary in the case of $\Phi(1, 1-x-i\eta, z)$. As an alternative to directly deriving each case independently, it can be shown that the series given above for $\Phi(1, 1-x-i\eta, z)$ is an analytic continuation of $\Phi(1, 1+x, z)$. This can be achieved by generalizing a theorem for analytic continuation of Laplace-type integrals.³³ Under more general hypotheses than those employed by Nikiforov and Uvarov,³³ the theorem allows analytic continuation of the series for $\Phi(1, 1+x, z)$ into the $\arg(x) < \pi$ region, subject to the condition $|x+z| > 0$. The $\eta \rightarrow 0$ limit can then be carried out as above. For the expansions to be useful, we require $|x+z| \gg 1$ and $|x-z| \gg 1$, which are satisfied for the physical regions investigated in Sec. IV.

- ¹*High Temperature Superconductivity*, edited by J. W. Lynn, Graduate Texts in Contemporary Physics (Springer-Verlag, New York, 1990), and the extensive list of references therein.
- ²M. R. Schafroth, *Phys. Rev.* **100**, 463 (1955). See also V. L. Ginzburg, *J. Stat. Phys.* **1**, 3 (1969).
- ³R. M. May, *Phys. Rev.* **115**, 254 (1959).
- ⁴R. M. May, *J. Math. Phys.* **6**, 1462 (1965).
- ⁵J. M. Blatt, *Theory of Superconductivity* (Academic, New York, 1964).
- ⁶F. Stern, *Phys. Rev. Lett.* **18**, 546 (1967).
- ⁷K. W. Chiu and J. J. Quinn, *Phys. Rev. B* **9**, 4724 (1974). For further work, see N. J. M. Horing and M. M. Yildiz, *Ann. Phys. (N.Y.)* **97**, 216 (1976); M. L. Glasser, *Phys. Rev. B* **28**, 4387 (1983).
- ⁸A. L. Fetter, *Ann. Phys. (N.Y.)* **81**, 367 (1973).
- ⁹A. L. Fetter, *Ann. Phys. (N.Y.)* **88**, 1 (1974).
- ¹⁰T. Ando, A. B. Fowler, and F. Stern, *Rev. Mod. Phys.* **54**, 437 (1982).
- ¹¹*Condensed Systems of Low Dimensionality*, edited by J. L. Beeby *et al.* (Plenum, New York, 1991).
- ¹²D. F. Hines and N. E. Frankel, *Phys. Rev. B* **20**, 972 (1979).
- ¹³E. G. Harris, in *Advances in Plasma Physics*, edited by A. Simon and W. B. Thompson (Wiley, New York, 1969), Vol. 3, p. 157.
- ¹⁴D. C. Bardos and N. E. Frankel, *Physica A* **189**, 282 (1992).
- ¹⁵N. S. Witte, V. Kowalenko, and K. C. Hines, *Phys. Rev. D* **38**, 3667 (1988); J. Daicic and N. E. Frankel, *Prog. Theor. Phys.* **88**, 1 (1992).
- ¹⁶I. S. Gradshteyn and I. M. Ryzhik, *Table of Integrals, Series and Products* (Academic, New York, 1980).
- ¹⁷I. B. Bernstein, *Phys. Rev.* **109**, 10 (1958).
- ¹⁸E. P. Gross, *Phys. Rev.* **82**, 232 (1951).
- ¹⁹J. P. Dougherty and J. J. Monaghan, *Proc. R. Soc. London, Ser. A* **289**, 214 (1965).
- ²⁰I. P. Shkarofsky and T. W. Johnston, *Phys. Rev. Lett.* **15**, 51 (1965).
- ²¹J. P. Dougherty and S. R. Watson in *Advances in Plasma Physics*, edited by A. Simon and W. B. Thompson (Wiley, New York, 1971), Vol. 4, p. 1.
- ²²N. J. Horing, *Ann. Phys. (N.Y.)* **31**, 1 (1965).
- ²³N. J. Horing and M. M. Yildiz, *Ann. Phys. (N.Y.)* **97**, 216 (1976).
- ²⁴D. C. Bardos and N. E. Frankel, following paper, *Phys. Rev. B* **49**, 4096 (1994).
- ²⁵D. F. Hines, Ph.D. thesis, Melbourne University, 1982.
- ²⁶S. R. Hore and N. E. Frankel, *Phys. Rev. B* **14**, 1952 (1976).
- ²⁷M. Abramowitz and I. A. Stegun, *Handbook of Mathematical Functions* (Dover, New York, 1965).
- ²⁸A. P. Prudnikov, Yu A. Brychkov, and O. I. Marichev, *Integrals and Series* (Gordon and Breach, New York, 1986), Vol. 2.
- ²⁹G. M. Walters and E. G. Harris, *Phys. Fluids* **11**, 112 (1968).
- ³⁰A. E. Delsante and N. E. Frankel, *Ann. Phys. (N.Y.)* **125**, 135 (1980).
- ³¹L. C. Slater, *Confluent Hypergeometric Functions* (Cambridge University Press, Cambridge, 1960).
- ³²B. C. Berndt, *Ramanujan's Notebooks Part I* (Springer, New York, 1985), p. 65.
- ³³A. F. Nikiforov and V. B. Uvarov, *Special Functions of Mathematical Physics* Birkhauser, Basel, 1988), Appendix B.